

Erik V. Bachtiar\*, Markus Rüggeberg and Peter Niemz

# Mechanical behavior of walnut (*Juglans regia* L.) and cherry (*Prunus avium* L.) wood in tension and compression in all anatomical directions. Revisiting the tensile/compressive stiffness ratios of wood

<https://doi.org/10.1515/hf-2017-0053>

Received April 19, 2017; accepted July 24, 2017; previously published online August 19, 2017

**Abstract:** The mechanical properties of walnut (*Juglans regia* L.) and cherry (*Prunus avium* L.) woods, as frequent raw materials in cultural heritage objects, have been investigated as a function of the anatomical directions and the moisture content (MC). The strength data are decreasing with increasing MC, whereas the tensile strength in the longitudinal direction is higher by factors of 1.5–2 compared to the compression strength. Moreover, the inequality of tensile and compressive stiffness is discussed, which is a matter of debate since a long time. This so-called bimodular behavior is difficult to describe in a generalized mode due to the high data variability if tension and compression properties are analyzed on different samples. If tensile and compressive stiffness tests are performed on the same samples of walnut and cherry wood, the ratio between these properties is significantly higher than 1.

**Keywords:** cherry wood (*Prunus avium* L.), stiffness ratios, strength ratios, tension and compression strengths, walnut wood (*Juglans regia* L.)

## Introduction

The mechanical properties of wood are of crucial importance in engineering applications. The knowledge in this field is limited to a very few wood species, mainly to those with high commercial value, in Europe for example to spruce (*Picea abies* L.) and beech (*Fagus sylvatica* L.) (Stamer and Sieglerschmidt 1933; Hörig 1935;

Keylwerth 1951). The experiments in this context are time consuming and complex, which is partly due to the orthotropic structure of wood (Bodig and Jayne 1993), the pronounced influence of moisture content (MC) on the mechanical properties (McBurney and Drow 1962; Gerhards 1982; Kollmann and Coté 1984) and the natural heterogeneity and variability of wood properties. Usually, a full characterization of one wood species includes nine independent elastic properties and six independent strength properties at three or more MC levels. A peculiarity is that tensile strength (TStr) in longitudinal (L) direction (TStr<sub>L</sub>) is considerably higher than the compressive strength (CStr<sub>L</sub>) because of the fibrous structure of wood (Kollmann and Coté 1984). A matter of discussion is whether and to which extent the tension and compression stiffnesses are different (Connors and Medvecz 1992). Thus, a comprehensive mechanical analysis should also include the stiffness data.

The hardwood species walnut (*Juglans regia* L.) and cherry (*Prunus avium* L.) are high value materials applied for woodturning, cabinets, furniture, and construction of musical instruments. Hence, a large part of historical objects found in the museums is made of these woods, which are hitherto not well characterized from the mechanical point of view. The fracture toughness of walnut and cherry were described in the perpendicular plane (Murata et al. 2017). The tension and compression loadings of these woods were often carried at one MC level and mainly in the L-direction (Keylwerth 1951; Nocetti et al. 2010; Korkut and Aytin 2015). Bachtiar et al. (2017) investigated mechanical parameters of these two wood species in all three anatomical directions at different MC levels and compared the data with those obtained by ultrasound measurements.

The current study is a continuation of the work of Bachtiar et al. (2017) aiming at the compression strength and tension strength data of walnut and cherry woods by taking into consideration all anatomical directions and several MC levels. The goal is to complete more the knowledge on the mechanical properties of these woods. The expectation is that the data will contribute to an improved conservation of art objects made of these woods, which are frequently found in museums. A complete data set

\*Corresponding author: Erik V. Bachtiar, Institute for Building Materials, ETH Zürich, 8093 Zürich, Switzerland, e-mail: berik@ethz.ch

Markus Rüggeberg: Institute for Building Materials, ETH Zürich, 8093 Zürich, Switzerland; and Laboratory of Applied Wood Materials, Empa, 8600 Dübendorf, Switzerland

Peter Niemz: Institute for Building Materials, ETH Zürich, 8093 Zürich, Switzerland; and Institute for Material and Wood Technology, Bern University of Applied Sciences, 6096 Biel, Switzerland

could also contribute to an advanced computational modeling (Zítek and Vyhliádal 2009; Konopka et al. 2016; Afshar et al. 2017) of walnut and cherry objects and could be helpful for a better understanding of the differences between tension and compression strength and the stiffness asymmetry of wood, in general.

## Materials and methods

**Abbreviations and symbols:** TStr and CStr are tension and compression strengths. TSt and CSt are tension and compression stiffnesses. TStr<sub>i</sub>, CStr<sub>i</sub>, TSt<sub>i</sub> and CSt<sub>i</sub> refer to  $i \in L, R$  and  $T$ , which are wood fiber in longitudinal, radial and tangential directions, respectively. MOE is modulus of elasticity. Moreover,  $\sigma$  and  $\varepsilon$  are stress and strain, and  $\sigma_y$  and  $\sigma_u$  are yield and maximum strengths. MC and RH are MC and relative humidity. Equilibrium moisture content (EMC) is the equilibrium moisture condition. FSP is the fiber saturation point. StD and coefficient of variance (CoV) are standard deviation and coefficient of variance, respectively. EW and LW are earlywood and latewood. Finally, MFA is the microfibril angle.

**Materials:** Walnut (*J. regia* L.) and cherry (*P. avium* L.) wood were taken from trees grown in the Caucasus region, east Europe. All specimens were free of defects, such as knots or heartwood. Under normal climatic conditions (65% RH, 20°C), the average densities of walnut and cherry wood are  $650 \pm 42 \text{ kg m}^{-3}$  and  $551 \pm 40 \text{ kg m}^{-3}$ , respectively.

**Specimen preparation:** Blocks with a dimension of  $100 \times 100 \times 500 \text{ mm}^3$  were stored at 0%, 65%, 85% and 95% RH at 20°C for at least 1 month prior to the specimen preparation. Dog-bone-shaped specimens (95 mm in length with a square cross-section of  $28 \times 28 \text{ mm}^2$ )

were prepared as usual (Keunecke et al. 2008; Hering et al. 2012; Ozyhar et al. 2013) for all mechanical tests performed in L-, R- and T-directions (Figure 1a) except for the tensile measurements in the L-direction. The middle part of the specimen (covering 11 mm in length) was shaped to a constant cross section of  $14 \times 14 \text{ mm}^2$  by a milling cutter. For the TStr<sub>L</sub> measurements, the sample geometry and dimension were chosen according to DIN-52188 (1979) (Figure 1b). For each experimental configuration and MC level, at least nine specimens were prepared. The samples were then further conditioned for another month to ensure a constant EMC.

**Density and MCs:** The density of the samples was measured before finishing the sample preparation, and the data are calculated as raw densities at specific MC levels. On the other hand, the MC was determined after finishing the experimental test on the fractured pieces. The data are presented based on oven dry weight according to the international standard ASTM-D143 (2014) by taking into consideration the average of at least 10 random pieces of wood obtained for each MC, i.e.

$$\%MC = 100(m_i - m_{od}) / m_{od}, \quad (1)$$

where  $m_i$  is the original mass measured as soon as the wooden piece was removed from the testing apparatus, and  $m_{od}$  is the oven dry mass measured after 24 h drying at 103°C.

**Mechanical tests:** The experimental tests were performed on a Universal Testing Machine (Zwick Roell Z100, Zwick Roell, Ulm, Germany) equipped with a 100-kN load cell. An initial force of 50 N was set as the starting point of the measurements. The tests were conducted in a displacement-controlled mode at a rate of  $1 \text{ mm min}^{-1}$ . Under these conditions, the failure occurs within  $90 \pm 30 \text{ s}$  (Keunecke et al. 2008). One-half of the dog-bone-shaped samples were tested in tension, the other in compression. Five successful

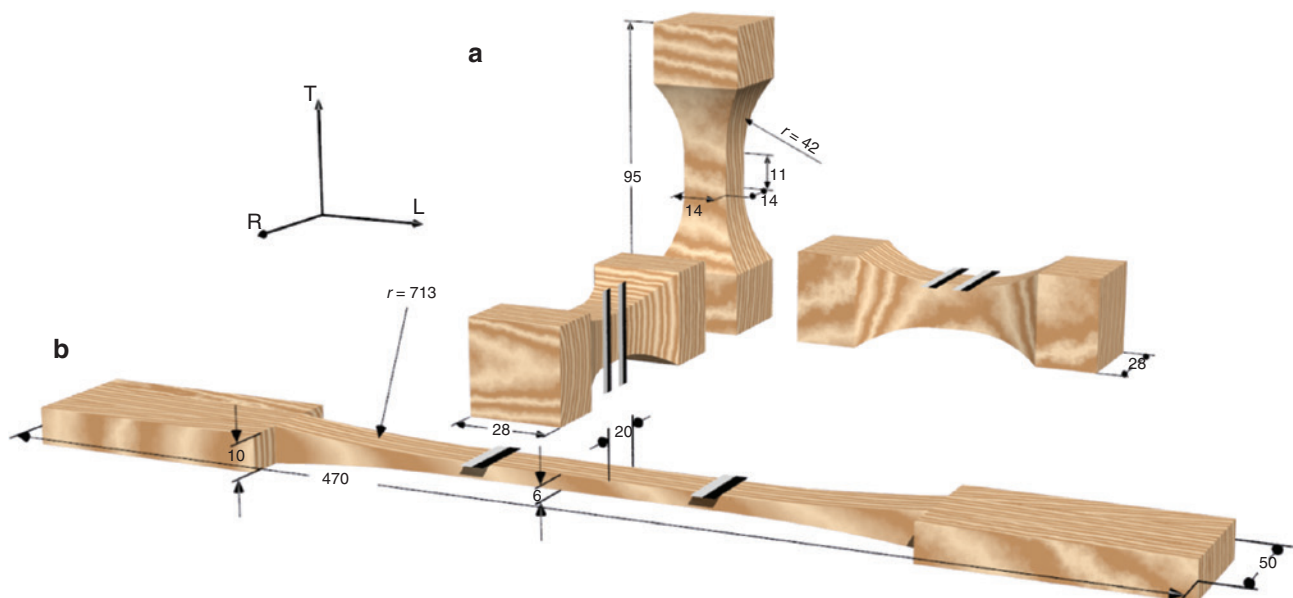


**Figure 1:** Sample geometry for mechanical tests with indicated black and white stripes for optical strain detection. (a) Dog-bone-shaped samples and (b) sample geometry for testing tensile strength in the L-direction. Dimensions are given in mm (DIN-52188 1979).

tests were obtained for each configuration with the exception of tensile tests on cherry wood in the T-direction at 65% RH, for which only four successful tests were obtained. In the L-direction, the dog-bone specimens were only tested in compression. For tension, as indicated above, 10 samples shown in Figure 1b were tested until failure. Hereby, the displacement was recorded by a camera via two black and white paper strips attached to the specimen. This technique is known as the video image correlation, which is directly integrated into the test and evaluation protocol of the Zwick machine. For more details, see Keunecke et al. (2008), Hering et al. (2012) and Ozyhar et al. (2013).

The failure criteria were defined based on Bodig and Jayne (1993). For tension in L-, R- and T-directions and compression in the L-direction, the maxima in stress (Figure 2) is followed by immediate failure. Hence, strength is directly taken as the maximum stress ( $\sigma_u$ ). No maximum stress can be observed for compression in R- and T-directions. The stress keeps increasing after the proportional limit of elasticity is reached. After a certain point, the strain attains an excessively large value (Figure 2) known as yield strength ( $\sigma_y$ ), which is defined as the failure criterion, which was also used in the current study. For yield strength, the stress at 0.2% plastic deformation was adopted from metallic materials (ASTM-E8/E8M-11 2011).

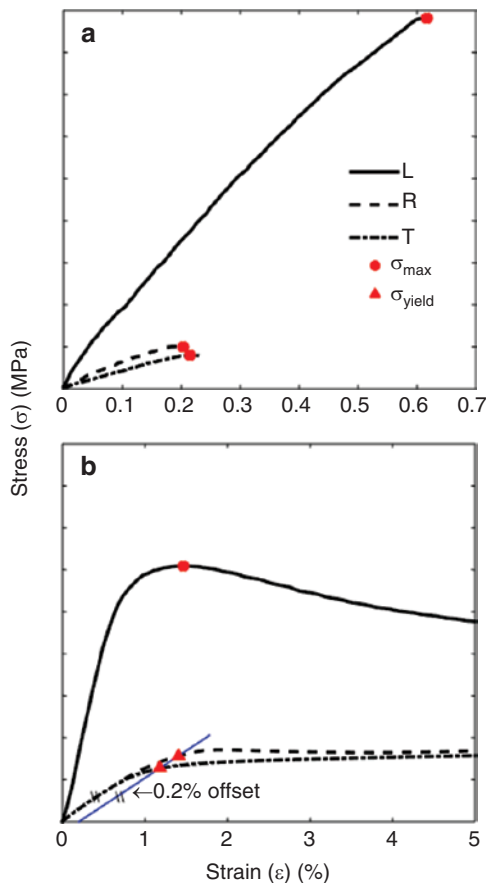


**Figure 2:** Stress-strain relations of wood under tension and compression loading and their failure criteria. (a) Tension and (b) compression.

**Statistical analysis:** The error propagation was taken into account. The second moment of the Taylor expansion (Benaroya et al. 2005) is used for calculating the standard deviations (StD) of the tension and compression ratio of the strength and stiffness data. For walnut and cherry wood, the stiffness ratio and its StD can be measured directly because the same specimens with known individual data are used. For the data of other studies, also with the same specimens, the StD calculation of the stiffness ratio requires the covariance of the data. This was not possible, as only the averages with StD values of the tension and compression data were available. The StD for the stiffness ratios of these data is likely to be overestimated when the covariance is assumed to be zero.

The data obtained were analyzed via t-test (significance level 0.05) with a pretest on the normal distribution of the data via Kolmogorov-Smirnov's test (Stephens 1974) and on the variance equality of each data pair via Bartlett's test (Snedecor and Cochran 1989) for the anatomical directions and MC levels. The stiffness data were tested via paired t-tests as the data are obtained from same specimens. On the other hand, all data, which are from different samples, are assumed to be uncorrelated and independent. As for the literature data of other wood species, which are only available as average values with StD, a suitable data set for a t-test is obtained by a series of a normally distributed random data, which were generated with the same number of specimens. This procedure was repeated 10 000 times and averaged, which ensures the consistent probability results. The whole statistical procedures are illustrated in Figure 3.

## Results and discussion

### Tensile and compressive strength

TStr and CStr are presented in Figure 4 and in Supplementary Data Table 1S. With values of  $89\% \pm 27\%$  MPa for walnut and  $105\% \pm 20\%$  MPa for cherry wood, the  $TStr_L$  is considerably higher than the  $CStr_L$ . For both wood species, these data are much higher than those measured in R- and T-directions. In L-, R- and T-directions, the strengths of walnut wood are lower by an average of 27%, 63% and 24% than those of cherry wood, respectively. In compression, however, the strength of walnut wood is only lower in the R-direction by an average of 17%. In the L-, and T-directions, the CStr values of walnut wood are on average 9% and 14% higher than the corresponding data of cherry wood.

In comparison with data of the U.S. Department of Agriculture (2010) concerning of black walnut (*Juglans nigra* L.) and black cherry (*Prunus serotina* Ehrh.) with 12% MC, the  $CStr_L$  data of the present study are 12% and 11% higher, respectively. The strength data of both species are also well in the range of those observed for other wood species with similar densities (Kretschmann 2010). Although the number of tested specimens in R- and T-directions is relatively low,

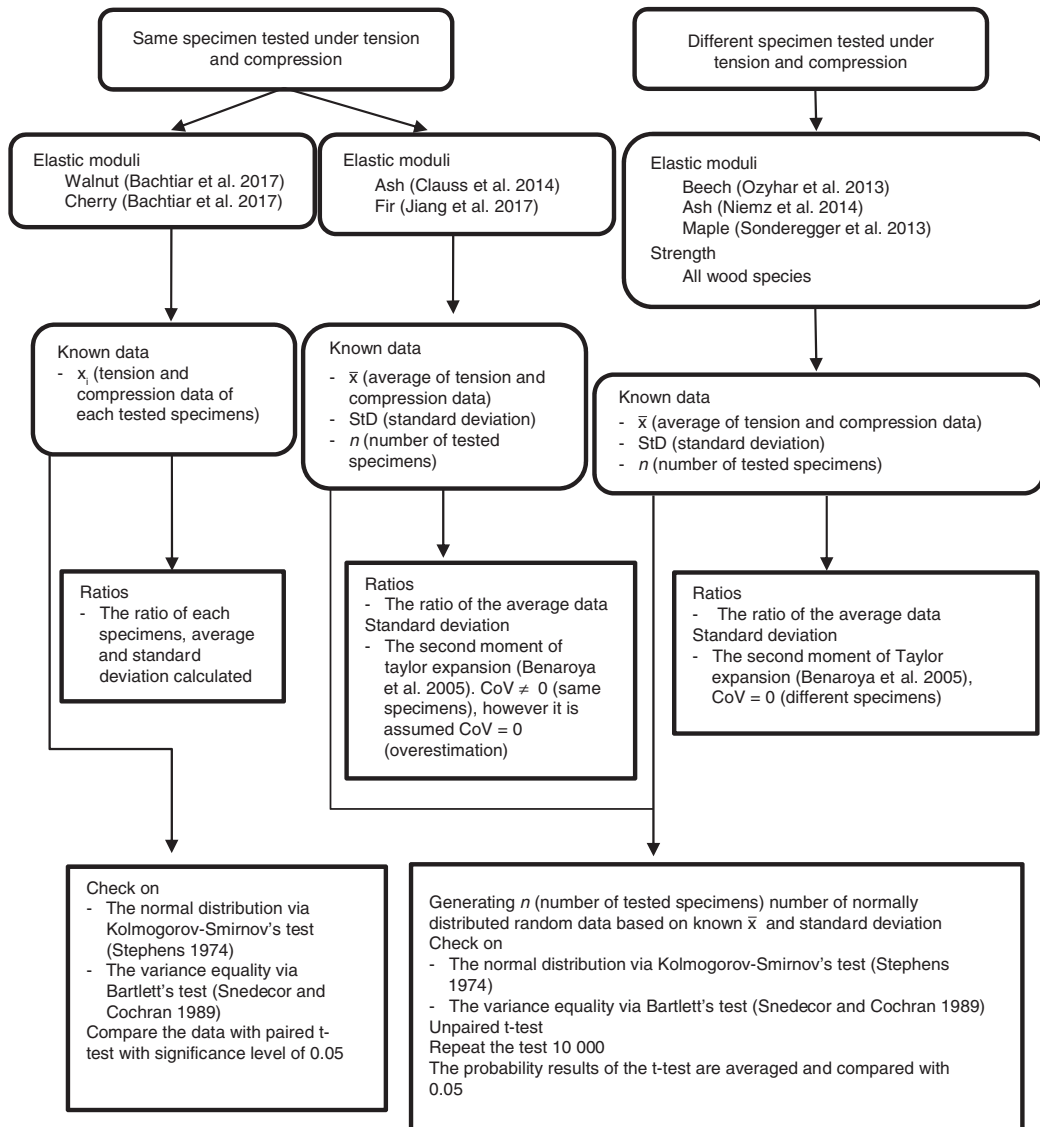


Figure 3: Flow chart for the statistical analysis measuring tension and compression ratio and their significance difference.

the CoV is also relatively low. This is an indication that a higher number of tested specimens would not improve the results essentially. In general, the data variation is low, when CStr tests in R- and T-directions result in prominent ductile failure, whereas the opposite is true in the case of brittle failure under tension.

### Data as a function of MC

The strengths data are decreasing with increasing MC in all anatomical direction for both TStr and CStr with exception of the TStr<sub>T</sub> data, which do not show a clear trend. Similar data dependency form MC is well known from the literature (Kollmann and Cote 1968; Gerhards 1982; Ozyhar

et al. 2012). This function is explained by the reduction of the number of hydrogen bonds, which are crosslinking the cellulose and other constituents in the non-crystalline regions of the cell walls with increasing MC (Winandy and Rowell 1984; Skaar 1988). A part of this effect is also due to the increase of the cross-sectional area due to swelling by water addition (Kollmann and Cote 1968), which leads to a lower calculated strength.

### Ratio of TStr to CStr in the L-direction

As described above, TStr<sub>L</sub> is considerably higher than CStr<sub>L</sub>. For walnut, a factor of around  $1.5\% \pm 27\%$  is calculated under normal climatic conditions, whereas a factor

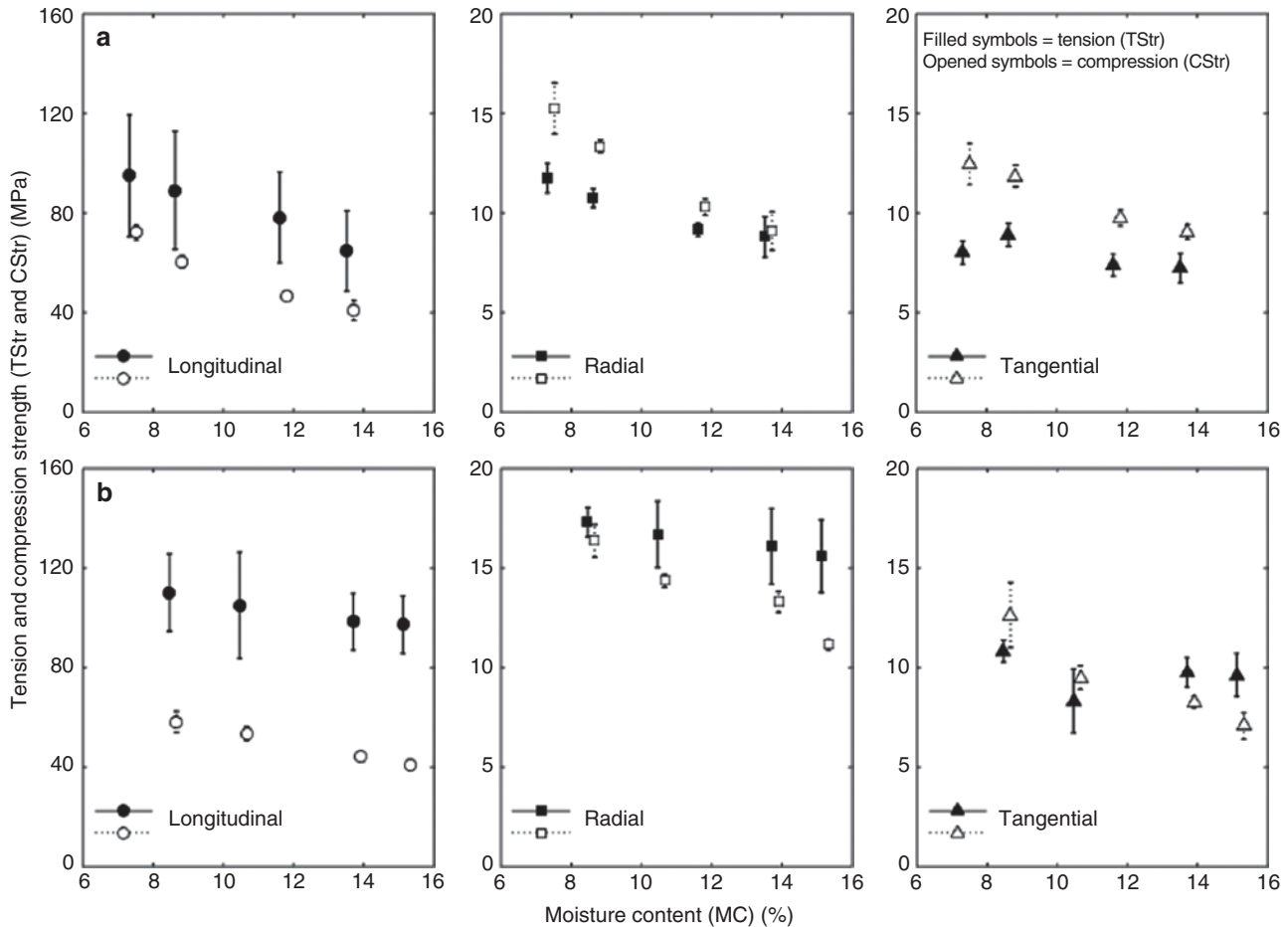


**Figure 4:** Moisture-dependent tension and compression strength (TStr and CStr) of: (a) walnut wood and (b) cherry wood. The compression data are presented with an offset of 0.2% moisture content.

of  $2.0\% \pm 21\%$  is calculated for cherry wood (Figure 5). The corresponding ratios are smaller in case of tests in the R- and T-directions. This behavior is well documented in the literature (Kollmann and Coté 1984). Figure 6 and Table 2S illustrate some literature data with this regard (Ozyhar et al. 2013; Sonderegger et al. 2013; Niemz et al. 2014; Jiang et al. 2017). In accordance to Kollmann and Coté (1984) concerning several hardwood and softwood species, it is seen that the TStr/CStr ratio varies for different wood species with an average factor of  $\approx 2$  at 12% MC. Clearly, the difference between TStr and CStr is due to the fibrous cellular structure of wood; while the fiber cells are being stretched under tension, they buckle under compression (Kollmann and Cote 1968; Bodig and Jayne 1993; Zauner et al. 2016).

In case of cherry wood and the other wood species, it is also clearly visible that  $TStr_L/CStr_L$  ratio increases with increasing MC up to 4 in the high MC range. For walnut wood, this factor is  $\approx 3$  already reaching the highest MC (Figure 5a). Concerning the MC effect, Ozyhar et al. (2013)

concluded that the strength asymmetry is driven mainly by the changes in the compression strength as a function of MC, i.e. the buckling of the fibers under compression is promoted more strongly by MC than the rupture under tension.

### Ratio TStr/CStr in R- and T-directions

Similar strength ratios are obtained for R- and T-directions (Figure 5). For walnut wood, the ratios are  $< 1$  at all MC levels, i.e.  $CStr > TStr$ . For cherry wood, ratios are  $\approx 1$ , which are increasing at higher MCs significantly. Interestingly, the CStr data are similar to walnut and cherry wood, whereas the TStr of walnut  $<$  TStr of cherry.

In Figure 6 and in Table 2S, the strength ratios of walnut and cherry wood are compared with literature data collected from various wood species, which were tested in all anatomical directions at 3 MC levels. For all species, the  $TStr_{R,T}/CStr_{R,T}$  ratios are  $< 1$ , and the data for R- and T-directions are closer to each other than those obtained

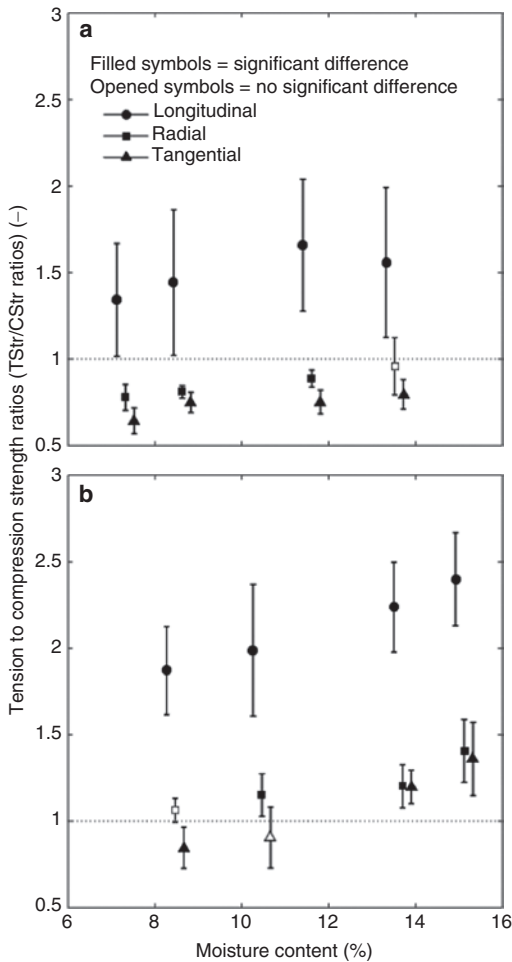


**Figure 5:** Moisture-dependent tension to compression strength ratios (TStr/CStr ratios) of (a) walnut wood and (b) cherry wood. The data of R and T are presented with a small offset in moisture content.

in the L-direction. However, the ratios  $TStr_R/TStr_T$  are mostly higher than 1.

It is obvious that in R- and T-directions, the fibrous structure of wood has only a minor influence. The failure under tension begins with the delamination of the cells via intrawall fracture between adjacent tracheids or fibers, or in association with rays or by trans-wall fractures exposing the cell lumens (Donaldson 2011). As wood cells are often aligned in radial files, R-delamination is associated with the intrawall fracture because of the weak link in the middle lamellae. In the T-direction, the middle lamellae do not form a straight lane, and therefore, the crack propagation goes through both the earlywood (EW) and latewood (LW). Thus, the delamination follows an irregular path, which consists of trans-wall fracture (often in thin walled EW) and intrawall fracture (mainly in thick walled LW or along the wood rays) depending on the less energy demand. In compression, on the other hand, yielding occurs by buckling before densification starts. The crucial aspect of this behavior is the thickness of the cell wall and the length of the cell wall along the loading direction. In the R-direction, the compression failure is often due to the crushing of an EW zone. In the T-direction, the compression failure is also partly crushing the EW. It continues between EW and LW in the T-direction, and the crushing of EW leads to the buckling of the growth ring (Bodig and Jayne 1993). Whether the ratios are higher or lower than 1 depends on the events occurring first, i.e. the buckling (due compressive yielding) or the rupture of trans-wall or intrawall (due to TStr).

The  $TStr_{R,T}/CStr_{R,T}$  ratio is also dependent on the way how the  $CStr_{R,T}$  is determined. Because of the absence of a

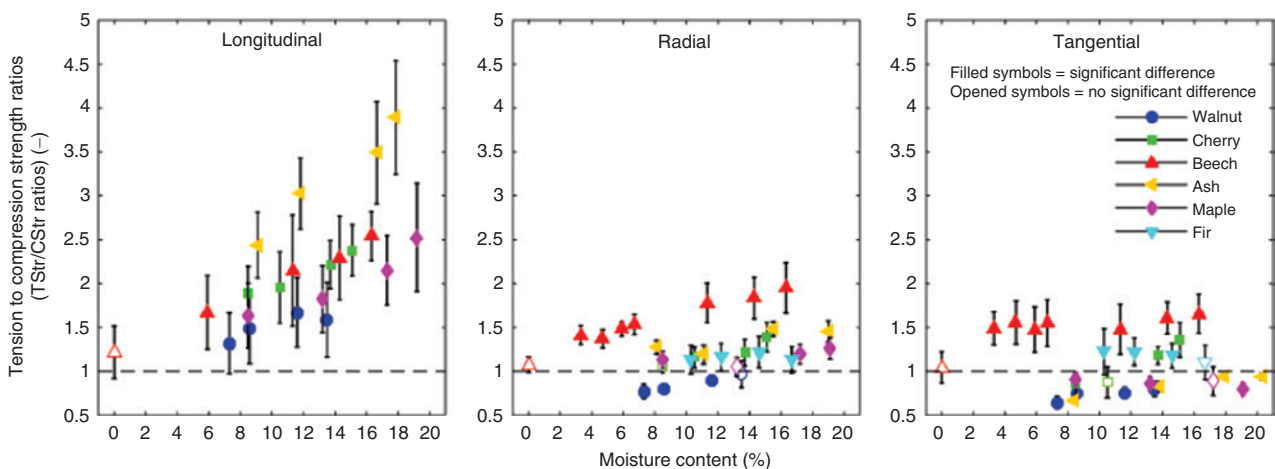


**Figure 6:** Moisture-dependent tension to compression strength ratios (TStr/CStr ratios) of different wood species: walnut and cherry wood (own measurement), beech wood (Ozyhar et al. 2013), ash wood (Niemz et al. 2014), maple wood (Sonderegger et al. 2013) and fir wood (Jiang et al. 2017) (see also Supplementary Table 2).

clearly visible maximum on the stress-strain curves, the actual value is dependent of the chosen failure criterion, which was fixed in the present study, as already mentioned, at the yield strength of 0.2% plastic deformation, which is adopted from failure criteria of steel (ASTM-E8/E8M-11 2011). In the case of 0.1% plastic deformation, for example, as failure criterion, the CSt<sub>r</sub> would decrease by an average of 12% ± 4% and 11% ± 2% in R- and T-directions, respectively. Thus, strength ratios may be either lower or higher than 1. For walnut and cherry wood, the  $TSt_{R,T}/CSt_{R,T}$  ratio would increase as a function of MC, as described for the L-direction, but up to four times less degree (Figure 6). Also here the ratios are MC dependent.

### Ratio of tension stiffness (TSt) to compression stiffness (CSt)

The stiffness data of both wood species for all three directions at different MC levels are provided by Bachtiar et al. (2017). The inequality between TSt and CSt, termed as bimodular behavior (Conners and Medvecz 1992), is a matter of discussion since a long time (Stern and Norris 1944; Sliker 1973; Bazan 1980; Conners 1985). Conners and Medvecz (1992) presented a data compilation from different wood species. The experiments and discussions in these studies have focused mainly on the L-direction and are mostly limited to one MC. The  $TSt_L/CSt_L$  ratios of various woods are in the range of 0.8–1.3, but data variations in detail concerning the wood species are not known.

In the study of Bachtiar et al. (2017), the TSt and CSt tests were performed on the same samples within the elastic regime in order to minimize the data scattering due to wood heterogeneity. Figure 7 illustrates the resulting TSt/CSt ratios for L-, R- and T-directions as a function of MC. With the exception of the L-direction at low MC, the ratios are significantly higher than 1 for both wood species and for all anatomical directions at different MC levels.

To contribute to the discussion about TSt/CSt ratios, a data compilation of several wood species is presented in Figure 8 and in Table 3S, including also data of walnut and cherry wood. In the studies of Bachtiar et al. (2017), Clauss et al. (2014) and Jiang et al. (2017) – where walnut, cherry, ash and fir wood were investigated – the same specimens were tested within the elastic range. These values are presented in Figure 8a for L-, R-, and T-directions, where TSt/CSt ratios are reliable because data scattering due to wood heterogeneity can be excluded. This situation is different to the data presented by Ozyhar et al. (2013), Sonderegger et al. (2013) and Niemz et al. (2014), where

different samples with different geometries were studied (Figure 8b). TSt data were obtained from dog-bone-shaped specimens (Figure 1a), whereas CSt data from wood blocks of 15 × 15 × 45 (L) mm<sup>3</sup> size.

For the same specimen, TSt/CSt ratios ≈ 1 or significantly higher than 1 were calculated for all three anatomical directions. Maximum ratios of up to 1.3% ± 6.3% were obtained for the L-direction, whereas ratios of up to 1.2% ± 6.3% were obtained for R- and T-directions. No correlation with MC is visible. Variability in stiffness and stiffness ratios is still present. In case of different specimens and sample geometries, or different experimental

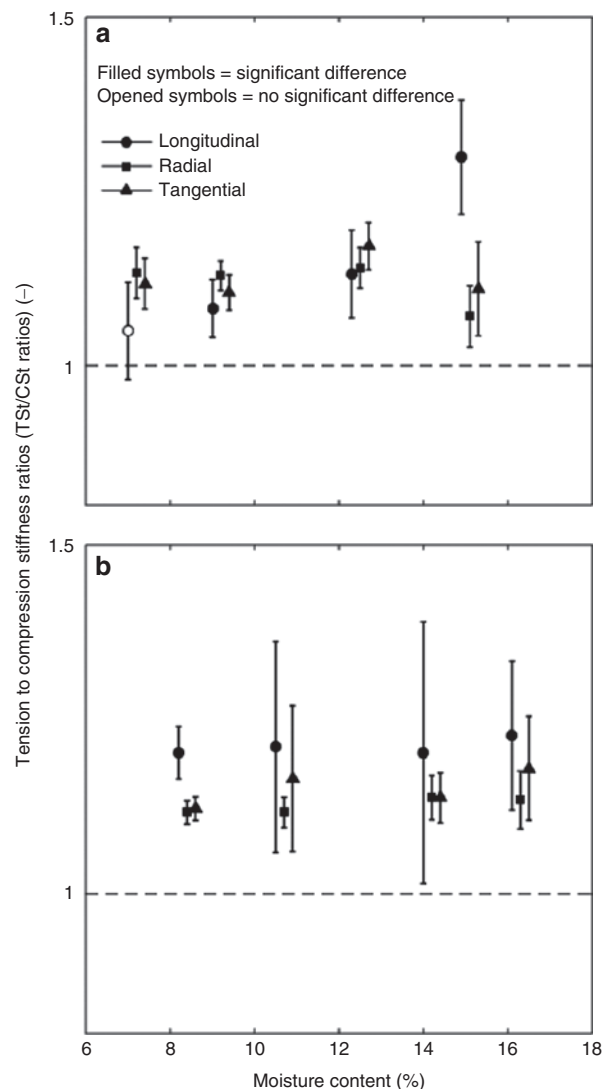


**Figure 7:** Moisture-dependent tension to compression stiffness ratios (TSt/CSt ratios) of (a) walnut wood and (b) cherry wood based on Bachtiar et al. (2017).

The data distributions are presented with an offset of -0.2%, 0% and 0.2% moisture content for longitudinal, radial and tangential directions, respectively.

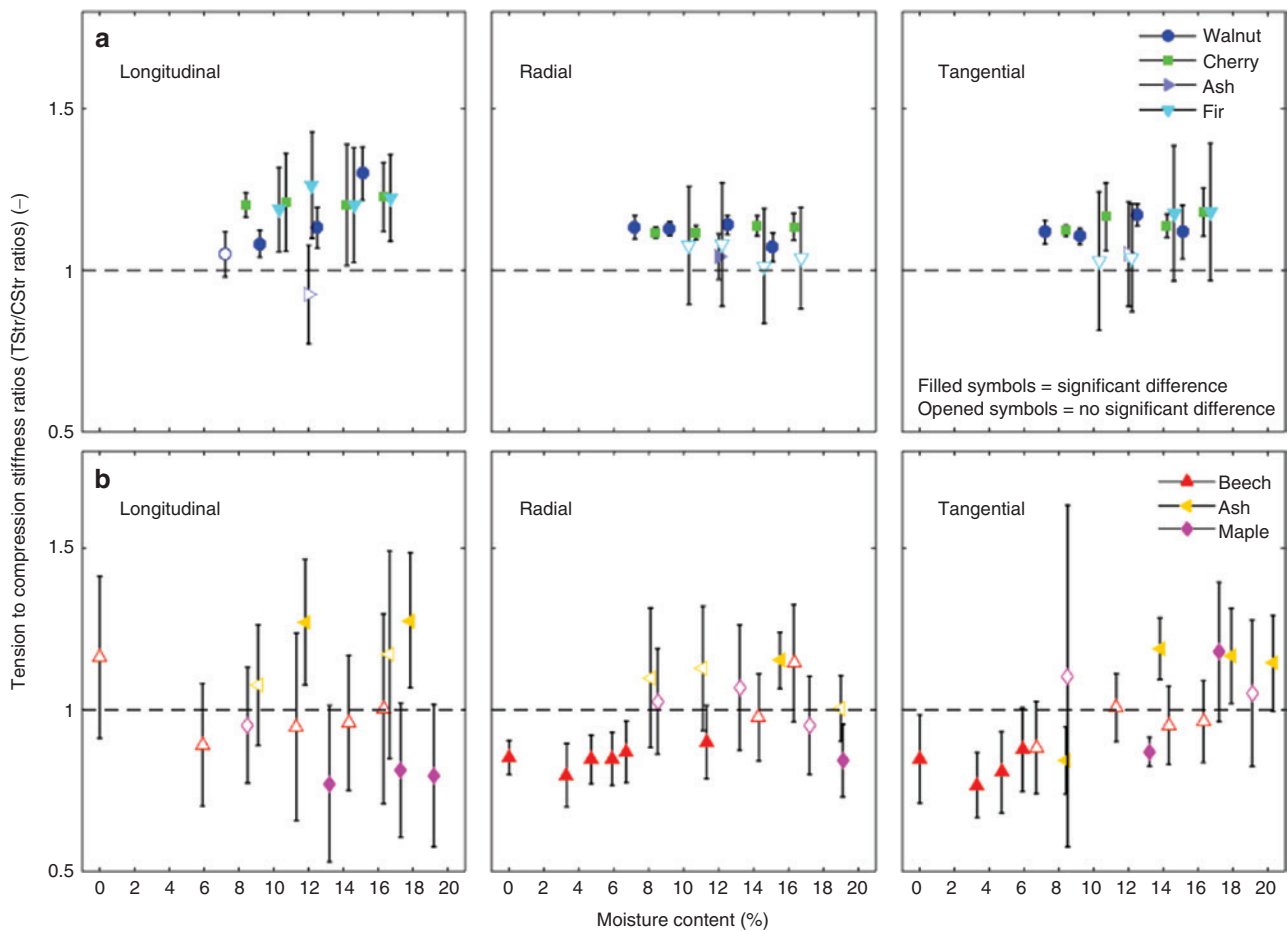


**Figure 8:** Moisture-dependent tension to compression ratios of stiffness (TSt/CSr ratios) based on the various studies: (a) same specimens tested under tension and compression, walnut wood (Bachtiar et al. 2017), cherry wood (Bachtiar et al. 2017), ash wood (Clauss et al. 2014) and fir wood (Jiang et al. 2017); (b) different specimens, beech wood (Ozyhar et al. 2013), ash wood (Niemz et al. 2014) and maple wood (Sonderegger et al. 2013) (see also Supplementary Table 3).

conditions, the resulting variation is considerably higher (Figure 8b). The averaged stiffness ratios are between 0.8 and 1.3, which is similar to that observed by Connors and Medvecz (1992). The majority of the calculated ratios are not significantly different from 1 (Figure 8b) except a few deviating data. As illustrated in Figure 8b, a reliable statement concerning the inequality of TSt and CSr is not possible in case of different samples and sample geometries. Thus, a real comparability with data of Connors and Medvecz (1992) is not given. The quoted authors explained TSt/CSr ratios >1 mainly based on the heterogeneity of composite biomaterials such as wood. For example, the wood fibers deviate from the strong parallelism because of the presence of wood rays, and thus the fibers may have a different behavior under loading in tension or compression. In the first case, this irregularity is of minor importance, but under compression, the buckling may be very different. The onset of the (reversible) buckling will lead to a

lower modulus of elasticity (MOE) under compression. The variation of the species-specific cellular structure is one of the influencing factors. However, based on the data of Wagenführ and Scheiber (1985) (Table 3S), the influence of wood rays is probably of less importance, as no correlation is visible between size and abundance of wood rays and the TSt/CSr ratios. Beech wood (*F. sylvatica* L.) with highest wood rays percentage (up to 21.2%) shows the lowest MOE<sub>L</sub> ratios, which are even lower than 1 in some cases.

The possible influence of microfibril angle (MFA) should also be taken into consideration. MFA strongly influences the stiffness as demonstrated by Gherardi Hein and Tarcísio Lima (2012), for example, for the compressive stiffness of *Eucalyptus* wood. If the MFA increases in the range between 8° and 23°, the CSr decreases. The gradient is 290 MPa per 1° of MFA. This dependency is different in case of TSt. It is assumed that in case of MFA increment above 0°, the TSt decreases moderately and CSr more



rapidly. If MFA is approaching 90°, the opposite behavior can be expected. The most common range of MFA in wood is less than 40° (Barnett and Bonham 2004; Gherardi Hein and Tarcísio Lima 2012; Wang et al. 2017), and in this range, the MFA influence on TSt is less pronounced than that in case of CSt leading to TSt > CSt. However, this is not a proven hypothetical behavior which is more probably for the L-direction. In the R- and T-directions, the MFA influence is expected to be essentially smaller.

## Conclusions

The tension strengths in longitudinal directions are higher by a factor of 1.5 and 2.1 for walnut and cherry wood compared to the compression strengths. MC influences the orthotropic material strength properties of these woods. If MC < FSP (fiber saturation point), the strength properties decrease. Concerning the ratios of tension to compression stiffnesses, it becomes clear that only data are reliable, which were obtained from the same sample, i.e. where the influence of wood's heterogeneity is excluded. The tensile to compressive stiffness ratios were significantly higher than 1, but a clear explanation about this so-called bimodularity cannot be given.

**Acknowledgements:** Funding through the Swiss National Science Foundation (project no. 14762) is gratefully acknowledged. Additionally, we want to thank Sven Schlegel and Thomas Schnider who helped during the specimen preparation.

## References

- Afshar, R., van Dijk, N.P., Bjurhager, I., Gamstedt, E.K. (2017) Comparison of experimental testing and finite element modelling of a replica of a section of the Vasa warship to identify the behaviour of structural joints. *Eng. Struct.* 147:62–76.
- ASTM-D143 (2014) Standard test methods for small clear specimens of timber. ASTM International, West Conshohocken, Pennsylvania, USA.
- ASTM-E8/E8M-11 (2011) Standard test methods for tension testing of metallic materials. ASTM International, West Conshohocken, Pennsylvania, USA.
- Bachtiar, E.V., Sanabria, S.J., Mittig, J.P., Niemz, P. (2017) Moisture-dependent elastic characteristics of walnut and cherry wood by means of mechanical and ultrasonic test incorporating three different ultrasound data evaluation techniques. *Wood Sci. Technol.* 51:47–67.
- Barnett, J., Bonham, V.A. (2004) Cellulose microfibril angle in the cell wall of wood fibres. *Biol. Rev.* 79:461–472.
- Bazan, I.M.M. (1980) Ultimate bending strength of timber beams. PhD dissertation in Civil Engineering, Nova Scotia Technical College, Halifax, Nova Scotia, Canada.
- Benaroya, H., Han, S.M., Nagurka, M. *Probability Models in Engineering and Science*. CRC Press, Florida, USA, 2005.
- Bodig, J., Jayne, B. *Mechanics of Wood and Wood Composites*. Krieger Publishing Company, Malabar, Florida, USA, 1993.
- Clauss, S., Pescatore, C., Niemz, P. (2014) Anisotropic elastic properties of common ash (*Fraxinus excelsior* L.). *Holzforschung* 68:941–949.
- Conners, T., Medvecz, C. (1992) Wood as a bimodular material. *Wood Fiber Sci.* 24:413–423.
- Conners, T.E. (1985) The effect of moisture gradients on the stiffness and strength of yellow-poplar. PhD dissertation in Forestry and Forest Products, Virginia Polytechnic Institute and State University, Blackburg, Virginia, USA.
- DIN-52188 (1979) Prüfung von Holz: Bestimmung der Zugfestigkeit parallel zur Faser. Beuth Verlag GmbH, Berlin, Germany.
- Donaldson, L. (2011) Delamination of wood at the microscopic scale: current knowledge and methods. In: *Delamination in Wood, Wood Products and Wood-Based Composites*. Ed. Bucur, V. Springer, Dordrecht, The Netherlands. pp. 123–144.
- Gerhards, C. (1982) Effect of moisture content and temperature on the mechanical properties of wood: an analysis of immediate effects. *Wood Fiber Sci.* 14:4–36.
- Gherardi Hein, P.R., Tarcísio Lima, J. (2012) Relationships between microfibril angle, modulus of elasticity and compressive strength in Eucalyptus wood. *Maderas Cienc. tecnol.* 14:267–274.
- Hering, S., Keunecke, D., Niemz, P. (2012) Moisture-dependent orthotropic elasticity of beech wood. *Wood Sci. Technol.* 46:927–938.
- Hörig, H. (1935) Anwendung der Elastizitätstheorie anisotroper Körper auf Messungen an Holz. *Ingenieur-Archiv* 6:8–14.
- Jiang, J., Bachtiar, E.V., Lu, J., Niemz, P. (2017) Moisture-dependent orthotropic elasticity and strength properties of Chinese fir wood. *Eur. J. Wood Wood Prod*, In print. Available at: <https://link.springer.com/article/10.1007/s00107-017-1166-y>.
- Keunecke, D., Hering, S., Niemz, P. (2008) Three-dimensional elastic behaviour of common yew and norway spruce. *Wood Sci. Technol.* 42:633–647.
- Keylwerth, R. (1951) The anisotropic elasticity of wood and plywood (Die anisotrope Elastizität des Holzes und der Lagenhölzer). Verlag des Vereins Deutscher Ingenieure. VDI-Forschungsheft 430:1–40.
- Kollmann, F.F.P., Cote, W.A. *Principles of Wood Science and Technology – Solid Wood*. Springer-Verlag, Berlin-Heidelberg, Germany, 1968.
- Kollmann, F.F.P., Coté, W.A. *Principles of Wood Science and Technology*. Springer-Verlag, Berlin, Germany, 1984.
- Konopka, D., Gebhardt, C., Kaliske, M. (2016) Numerical modelling of wooden structures. *J. Cult. Herit.* In print. <http://doi.org/10.1016/j.culher.2015.09.008>.
- Korkut, S., Aytin, A. (2015) Evaluation of physical and mechanical properties of wild cherry wood heat-treated using the thermowood process. *Maderas Cienc. Tecnol.* 17:171–178.
- Kretschmann, D.E. (2010) Mechanical properties of wood. In: *Wood Handbook: Wood as an Engineering Material*. Ed. Ross, R.J. U.S. Department of Agriculture, Forest Service, Forest Products Laboratory, Madison, Wisconsin, USA. pp. 5.1–5.46.
- McBurney, R., Drow, J. (1962) The elastic properties of wood: young's moduli and poisson's ratios of douglas-fir and their relations to moisture content. Technical Report No. 1528-D.

- United States Department of Agriculture, Forest Service, Forest Products Laboratory Madison, Wisconsin, USA.
- Murata, K., Bachtiar, E.V., Niemz, P. (2017) Determination of mode I and mode II fracture toughness of walnut and cherry in TR and RT crack propagation system by the Arcan test. *Holzforschung* 71:985–990.
- Niemz, P., Clauss, S., Michel, F., Hänsch, D., Hänsel, A. (2014) Physical and mechanical properties of common ash (*Fraxinus excelsior* L.) *Wood Res.* 59:671–682.
- Nocetti, M., Brunetti, M., Ducci, F., Romagnoli, M., Santi, F. (2010) Variability of wood properties in two wild cherry clonal trials. *Wood Sci. Technol.* 44:621–637.
- Ozyhar, T., Hering, S., Niemz, P. (2012) Moisture-dependent elastic and strength anisotropy of european beech wood in tension. *J. Mater. Sci.* 47:6141–6150.
- Ozyhar, T., Hering, S., Niemz, P. (2013) Moisture-dependent orthotropic tension-compression asymmetry of wood. *Holzforschung* 67:395–404.
- Skaar, C. *Wood-Water Relations*. Springer-Verlag, New York, USA, 1988.
- Sliker, A. (1973) Young's modulus parallel to the grain in wood as a function of strain rate, stress level and mode of loading. *Wood Fiber Sci.* 4:325–333.
- Snedecor, G., Cochran, W. *Statistical Methods*. Eight Ed. Iowa University Press, Ames, Iowa City, Iowa, USA, 1989.
- Sonderegger, W., Martienssen, A., Nitsche, C., Ozyhar, T., Kaliske, M., Niemz, P. (2013) Investigations on the physical and mechanical behaviour of sycamore maple (*Acer pseudoplatanus* L.). *Eur. J. Wood Wood Prod.* 71:91–99.
- Stamer, J., Sieglerschmidt, H. (1933) Elastische Formänderung der Hölzer. *Z. Ver. Dtsch. Ing.* 77:503–505.
- Stephens, M.A. (1974) EDF statistics for goodness of fit and some comparisons. *J. Am. Stat. Assoc.* 69:730–737.
- Stern, E.G., Norris, E.B. (1944) Strength properties of yellow poplar from Virginia. *Bull. Va. Polytech. Inst.* 38:3–34.
- Wagenführ, R., Scheiber, C. *Holzatlas*. Fachbuchverlag Leipzig, Leipzig, Germany, 1985.
- Wang, H., Yu, Z., Zhang, X., Ren, D., Yu, Y. (2017) The combined effects of initial microfibrillar angle and moisture contents on the tensile mechanical properties and angle alteration of wood foils during tension. *Holzforschung* 71:491–497.
- Winandy, J.E., Rowell, R.M. (1984) The chemistry of solid wood. In: *Advances in Chemistry Series (Volume 207)*. Ed. Roger Rowell, ACS Publications. US. Department of Agriculture: <http://pubs.acs.org/isbn/9780841207967>.
- Zauner, M., Stampanoni, M., Niemz, P. (2016) Failure and failure mechanisms of wood during longitudinal compression monitored by synchrotron micro-computed tomography. *Holz-forschung* 70:179–185.
- Zítek, P., Vyhliđal, T. (2009) Model-based moisture sorption stabilization in historical buildings. *Build Environ.* 44:1181–1187.

---

**Supplemental Material:** The online version of this article offers supplementary material (<https://doi.org/10.1515/hf-2017-0053>).